Laser-driven ablation through fast electrons in PALS experiment

S.Yu. Gus'kov[1,a], T. Chodukowski[2] , N. Demchenko[1], Z. Kalinowska[2], A. Kasperczuk[2], E. Krousky[3], M. Pfeifer[3], P. Pisarczyk[4], T. Pisarczyk[2], O. Renner[3], J. Skala[3], M. Smid[3], J. Ullschmied[5]

[1]P.N.Lebedev Physical Institute of RAS, 119991 Leninskii pr. 53, Moscow, Russia
[2]Institute of Plasma Physics and Laser Microfusion, 23 Hery St., 00-908 Warsaw, Poland
[3]Institute of Physics ASCR, v.v.i., Na Slovance 2, 182 21 Prague 8, Czech Republic
[4]Warsaw University of Technology, ICS, 15/19 Nowowiejska St., 00-665 Warsaw, Poland
[5]Institute of Plasma Physics ASCR, v.v.i., Za Slovankou 3, 182 00 Prague 8, Czech Republic

Abstract. Energy transfer to shock wave in Al and Cu targets irradiated by a laser pulse with intensity of I≈1-50 PW/cm^2 and duration of 250 ps was investigated at Prague Asterix Laser System (PALS). The iodine laser provided energy in the range of 100-600 J at the first and third harmonic frequencies. The focal spot radius of laser beam on the target was varied from 160 to 40 μm. The dominant contribution of fast electron energy transfer into the ablation process was found when using the first harmonic radiation, the focal spot radius of 40-100 μm, and the energy of 300-600 J. The fast electron heating results in the growth of ablation pressure from 60 Mbar at the intensity of 10 PW/cm^2 to 180 Mbar at the intensity of 50 PW/cm^2 and in the growth of the efficiency of the energy conversion into the shock wave from 2 to 7 % under the conditions of 2D ablation.

1 Introduction

The one of the subjects related to shock ignition method (SI) [1,2] that is influence of fast electron energy transport in laser-produced plasma on efficiency of energy coupling to shock wave in a dense target is studied. In the experiments the coupling parameter $I\lambda^2$ (I and λ are the intensity and wave length of laser radiation) was varied in the range of 10^{14}-8×10^{16} Wμm^2/cm^2 (low to high level of fast electrons effect) at the laser pulse intensity (1-50 PW/cm^2) and duration (250 ps) close to that at SI. In the case of relatively short plasma of PALS experiments the fast electrons are generated due to TNSA mechanism near the plasma resonance region, while in the case of the SI extended plasma the fast electrons are generated due to stimulated parametric processes in the lower density plasma. Nevertheless as shown below, the average energy of fast electrons in the high intensity PALS experiments is close to that measured in the OMEGA laser SI experiments [3]. Under the action of tightly focused laser beam the expansion of laser-produced plasma is not planar, therefore the interpretation of the results was based on 2D numerical simulations and analytical model taking into

[a] e-mail : guskov@sci.lebedev.ru

account the lateral expansion of ablated material. To determine plasma density and temperature a 3-frame interferometry and an x-ray spectroscopy were used. The laser energy transferred to the solid target was determined via measurements of the crater volume created on the target surface.

2 Experiment

The experiments were carried out at a normal incidence of the PALS laser radiation of the first (λ_1 = 1.315 μm) and third (λ_3 = 0.438 μm) harmonics on a surface of planar Al or Cu targets. The pulses of 120, 290, and 580 J energies (in the 3ω case only two first energies were available) with duration of 250 ps (FWHM) were applied. The values of beam radii (R_L) of 40, 80, 120 and 160 μm provided the variation of the incident laser intensity on the target, for example at the laser energy E_L=290 J, from $I_L=1.4\times10^{15}$ (R_L=160 μm) to $I_L=2.3\times10^{16}$ W/cm^2 (R_L=40 μm). The maximum value of the coupling parameter $I\lambda^2(8\times10^{16}$ Wμm^2/cm^2) was achieved at the energy of 580 J for 1ω and R_L=40 μm while its minimum value (1.1×10^{14} Wμm^2/cm^2) – at the energy of 120 J for 3ω and R_L=160 μm.

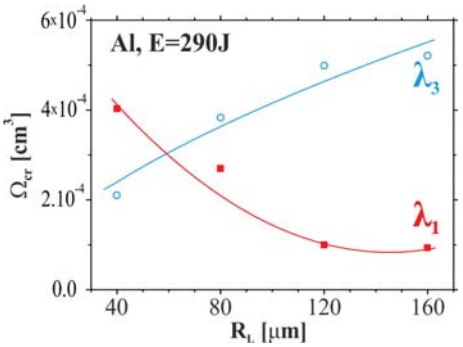

Fig. 1. Volume of the crater vs the beam radius at the energy of 290 J of the first and third harmonics laser radiation for Al target.

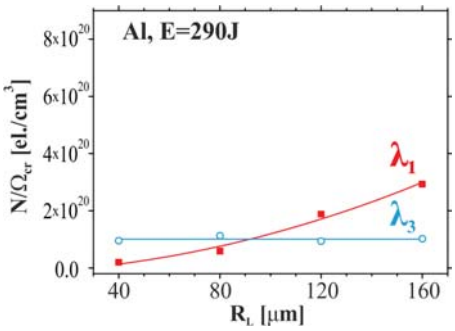

Fig. 2. Ratio of electron number to crater volume vs the beam radius at the energy of 290 J of the first and third harmonics of the laser radiation for Al target

The dependencies of the crater volume Ω_{cr} produced in Al target and the ratio of total number of plasma electrons N_e (computed on the basis of interferometric measurements of spatial electron density distribution) to crater volume on the laser beam radius are presented in Figs. 1 and 2.

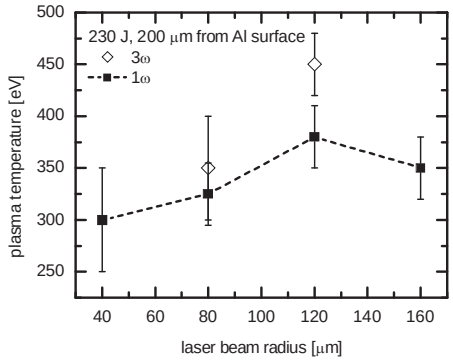

Fig. 3. Plasma temperatures at the distance of 200 μm from Al target surface irradiated at different laser harmonics and focal radii at the laser energy of 230 J.

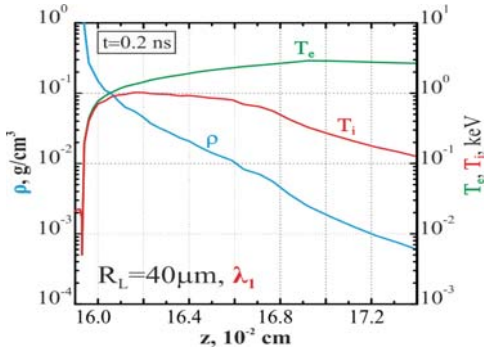

Fig. 4. Distributions of mass density, electron and ion temperatures on the axis of the plasma for Al target irradiated by the first harmonic beam at 40 μm radius

The data of both figures correspond to experiments with the energy of 290 J of the 1ω and 3ω laser radiation. The similar results were obtained for Cu target. In the 3ω case, the crater volume (energy transferred to the solid target) decreases with the decreasing R_L despite the increasing intensity of the laser beam that is explained by lateral expansion of the laser-produced plasma at the negligible role of fast electron energy transfer. By contrast, in the 1ω case, when at the given intensity the coupling parameter $I\lambda^2$ is 9 times larger than in the 3ω case, the crater volume increases with the decreasing R_L (increasing intensity), particularly fast in the range of small radii of 40-100 μm (large values of $I_L\lambda^2$). This fact points out to appear an additional factor of energy transfer, which is stronger than the

lateral expansion effect, that it is natural to associate with energy transfer by fast electrons. The same conclusion follows from the data of Fig. 2, which show decreasing the number of electrons providing the creation of the unit crater volume with decreasing R_L in the 1ω case.

The plasma temperatures spectroscopically measured at the distance of 200 μm from Al target surface irradiated by 230 J of the 1ω and 3ω laser radiation are presented in Fig. 3. The temperature decrease at the small radii of 1ω beam indicates the heating depth growth with increasing intensity. Temperature in the case of 3ω beam is by a factor of 1.2-1.3 higher than that in the case of 1ω beam.

3 Numerical simulation and model

The numerical simulations of the laser beam interaction with Al target were carried out for the energy of 290 J of the first and third harmonics laser beam with the radii 120 and 40 μm using the 2D hydrodynamic code ATLANT-HE. The code includes refraction of the laser radiation in the plasma, inverse bremsstrahlung and resonance mechanisms of the laser light absorption, fast electron generation due to the resonance absorption and its energy transfer with Coulomb collisions. The results of simulations are the following. In the 1ω case and R=120 μm (I_L=2.6×10^{15} W/cm^2): total absorption coefficient is K_a=0.38, absorption coefficient due to resonant mechanism is K_{ra}=0.08, fast electron temperature T_h=14 keV, crater volume Ω_{cr}=1.7×10^{-4} cm^3; in the 1ω case and R=40 μm (I_L=2.3×10^{16} W/cm^2): K_a=0.28, K_{ra}=0.06, T_h=90 keV, Ω_{cr}=4.1×10^{-4} cm^3. In the 3ω case and R=120 μm (I_L=2.6×10^{15} W/cm^2): K_a=086, K_{ra}=0.07, T_h=3 keV, Ω_{cr}=2.4×10^{-4} cm^3; in the 1ω case and R=40 μm (I_L=2.3×10^{16} W/cm^2): K_a=0.73, K_{ra}=0.1, T_h=19 keV, Ω_{cr}=1.8×10^{-4} cm^3. In the Fig. 4 the dependences of mass density, electron and ion temperatures on the beam radius are presented.

The analytical model is developed to explain the results of experiments and simulations. It combines the 1D and 3D self-similar solutions for isothermal expansion of a given mass of material [4] by means introducing the parameter, which is ratio of laser-produced plasma size and laser beam radius. The plasma density (ρ_a), temperature (T_a) and pressure (P_a) on the ablation surface as well as the efficiency of energy transfer (σ) to shock wave propagating and creating the crater in a solid target (ablation loading efficiency) determined by the ablation pressure, according this model, are

$$\rho=\frac{3\mu^{3/2}}{(2\pi)^{1/2}I^{1/2}\tau^{3/2}}\Psi^{-2},\quad T=\frac{I\tau}{2C_V\mu\left(2-\Psi^{-1}\right)},\quad P=\frac{I^{1/2}\mu^{1/2}}{\left(2\pi\right)^{1/2}\tau^{1/2}\left[\Psi\left(2\Psi-1\right)\right]} \qquad (1)$$

$$\sigma=\frac{2^{1/2}\mu^{3/4}}{\left(2\pi\right)^{3/4}\left(\gamma+1\right)^{1/2}I^{1/4}\tau^{3/4}\rho_0^{1/2}}\frac{\Psi^{1/2}}{\left(2\Psi-1\right)^{3/2}} \qquad (2)$$

where μ is the areal ablated mass, which is determined either by the depth of matter heating by thermal conductivity wave (μ_c), or by the range of fast electrons (μ_e)

$$\mu_c=\frac{\kappa^{1/3}I^{2/3}\tau^{2/3}}{C_V^{7/6}}\approx 2.6\cdot10^{-3}\frac{A^{7/6}I_{(pw)}^{2/3}t_{(ns)}^{2/3}}{(Z+1)^{7/6}\left(Z+3.3\right)^{1/3}},\ \mu_e=\frac{E_0^2\cdot A\cdot m_p}{4\pi e^4\cdot Z\cdot\Lambda}\approx 5.2\cdot10^{-7}\frac{A}{Z}E_{0(keV)}^2\ \text{g/cm}^2 \qquad (3)$$

the electron conductivity coefficient (at the value of Coulomb logarithm Λ=5) κ=8.4×10^{19}/(Z+3.3) erg×cm^{-1}×s^{-1}×keV$^{-7/2}$ and $E_{0(\text{keV})}$= 8($I_{L(pw)}\lambda_\mu^2$)$^{2/3}$ (the values $I_{(pw)}$ and $I_{L(pw)}$, $\tau_{(ns)}$, λ_μ are measured, respectively, in the units of 10^{15} W/cm^2, ns, μm); $I=K_aI_L$ is the absorbed radiation intensity; C_V = $Zk_B/Am_p(\gamma-1)$ is specific heat; γ is adiabatic exponent, Z and A are the charge and atomic number of the plasma ions, k_B is the Boltzmann constant, m_p is the proton mass, $\Psi=(1+2^{3/4}L_p/3R)$ is the factor of lateral plasma expansion; $L_p=(I\tau^3/\mu)^{1/2}$ is the plasma size; ρ_0 is the initial density of target material. Under conditions of considered experiments, according to (3), in the 3 ω case $\mu_c>\mu_e$ for all radii,

while in the 1ω case $\mu_c>\mu_e$ for the radii R=160 and 120 μm and $\mu_c<\mu_e$ for the radii R = 80 and 40μm. The results of calculations of ablation loading efficiency as well as volume of crater $\Omega_{cr}=\sigma K_a E_L/\alpha\varepsilon\rho_s$ ($\varepsilon=2.6\times10^3$ J/g is the specific energy for evaporation of unit mass of Al target, α=1.5 is the ratio between the thermal and kinetic energy of shock wave) are presented in Fig. 5 and 6. According to (3), the fast electron transfer provides a stronger growth of ablated mass and, consequently, stronger growth of the ablation density with increasing the laser intensity than thermal conductivity wave. At the beam radii of 160 and 120 μm the ablation is provided by thermal conductivity and the lateral expansion effect is negligible for both harmonics. Therefore, $\rho_{a(c)}\propto I^{1/2}$ and for given laser intensity $\sigma_{(c)}\propto K_a^{1/4}R^{-1/2}$, $\Omega_{cr}\propto K_a^{5/4}R^{-1/2}$. Thus, for large beam radii at both harmonics crater volume depends weakly on radius, and the ratio of the crater volumes in the 3ω and 1ω cases equals approximately to the ratio of the absorption coefficients: $\Omega_{cr(3)}/\Omega_{cr(1)}\approx(K_{a(3)}/K_{a(1)})^{5/4}$. At the small beam radii of 80 and 40 μm the lateral expansion effect is strong and, therefore, $\rho/\rho_a\propto(R/L)^2\propto R^2\mu/I$. From here we get follows $\rho_{(e)}/\rho_{a(e)}\propto R^{4/3}K_a^{1/3}$ and $\rho_{(c)}/\rho_{a(c)}\propto R^{8/3}K_a^{-1/3}$. So in the 3ω case, when ablation, as before, is provided by thermal conductivity $\sigma_{(c)}\propto K_a^{1/12}R^{-5/6}$ and $V_{cr}\propto K_a^{13/12}R^{5/6}$. In the 1ω case, i.e at ablation due to fast electron heating $\sigma_{(e)}\propto K_a^{11/12}R^{-5/6}$ and $V_{cr}\propto K_a^{23/12}R^{-5/6}$.

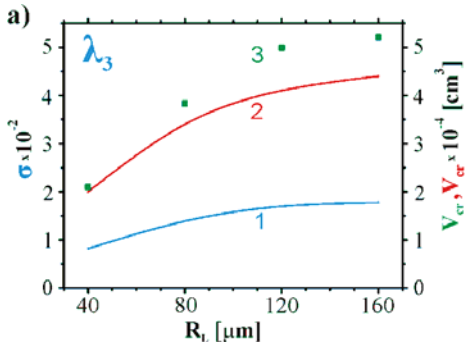

Fig. 5. Ablation loading efficiency (curve 1) and theoretical (curve 2) and experimental values (curve 3, green squares) of crater volume vs focal spot radius at energy of 290 J of the 3ω radiation.

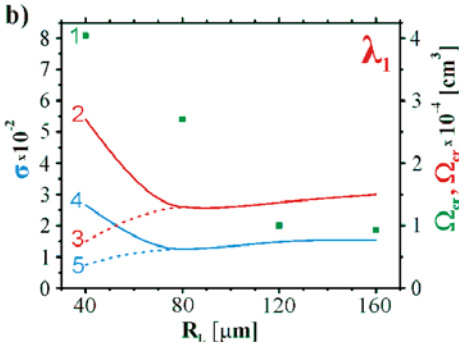

Fig. 6. Experimental (curve 1, green squares) and theoretical crater volume with (curve 2) and without (curve 3) taking into account the fast electron transport and ablation loading efficiency with (curve 4) and without (curve 5) taking into account the fast electron transport vs the beam radius at the energy of 290 J of the 1ω radiation.

4 Conclusion

At the laser intensity of 10-50 PW/cm^2 and $I\lambda^2=10^{16}$-5×10^{16} Wμm^2/cm^2 (the experiments with the laser pulse energy of 290-580 J for the first harmonic of iodine laser radiation) relevant to the laser spike in SI approach the dominant mechanism of ablation during the period of 250 ps is the matter heating by fast electrons. In spite of the lateral expansion, the ablative pressure increases from 100 Mbar for the intensity of 10 PW/cm^2 to 300 Mbar for the intensity of 50 PW/cm^2, whereas the efficiency of the laser energy transformation into the shock wave energy is on the level of 2-7%.

This work was supported by RFBR projects No 12-02-92101-JF and No 11- and 13-02-00295, by the Czech Republic AS project M100101208 and by the Czech Science Foundation project CZ.1.07/2.3.00/20.0279 and by the NCN of Poland Grant No 2012/04/M/ST2/00452.

References

1. V.A. Scherbakov, Sov. J. Plasma Phys. **9**, 240 (1983)
2. R. Betti, C.D. Zhou, K.S. Anderson et al, Phys. Rev. Lett. **98**, 155001 (2007)
3. W. Theobald, R. Nora, M. Lafon et all, Phys. Plasmas **19,** 102706 (2012)
4. V.S. Imshennik. Sov. Phys. Dokl. **5**, 263 (1960)